COBEM 2023 27TH INTERNATIONAL CONGRESS OF MECHANICAL ENGENEERING

ABCM Brazilian Society of Mechanical Sciences and Engineering
27th ABCM International Congress of Mechanical Engineering
December 04-08, 2023, Florianópolis-SC, Brazil

COB-2023-0731
VSPKC MICROMECHANICAL MODEL – A NOVEL ROM-BASED APPROACH

Lucas L. Vignoli
Center for Technology and Applications of Composite Materials, Department of Mechanical Engineering, Universidade Federal do Rio de Janeiro, Macaé, RJ, Brazil
ll.vignoli@mecanica.coppe.ufrj.br

Marcelo A. Savi
Center for Nonlinear Mechanics, COPPE – Department of Mechanical Engineering Universidade Federal do Rio de Janeiro, RJ, Brazil
savi@mecanica.coppe.ufrj.br

Pedro M.C.L. Pacheco
Department of Mechanical Engineering, Centro Federal de Educação Tecnológica Celso Suckow da Fonseca CEFET/RJ, Rio de Janeiro, RJ, Brazil
pedro.pacheco@cefet-rj.br

Alexander L. Kalamkarov
Department of Mechanical Engineering, Dalhousie University, Halifax, Nova Scotia, Canada, B3H 4R2
alex.kalamkarov@dal.ca

Abstract. *The design of composite structures is a multiscale challenge, from micro to macroscale. Concerning this multiscale characteristic, a large number of variables are involved and analytical approaches become fundamental tools for optimization procedures. The importance to estimate the effective macromechanical response of the composite using just the constituents' properties is unquestionable, decreasing the requirement of experimental tests. The present study aims to develop a novel micromechanical model, namely VSPKc, to estimate the effective elastic properties of unidirectional laminae. Solid mechanical arguments are considered adopting parallel and series associations of elements to define the micromechanical distribution of macromechanical loads. The proposed approach is based on the rule of mixture and considers the unit cell symmetry and a fiber with circular cross section geometry. A set of closed-form equations are derived, resulting in an efficient model with simple implementation and without the need to calibrate any empirical parameter. Finite element simulations using the commercial software Ansys and experimental data are employed as reference solutions in order to verify the model capability to estimate the elastic properties. On this basis, 126 experimental data are compiled from the literature. Other analytical models from the literature are compared with the proposed model that the VSPKc presented the best results concerning both metric, experimental data and finite element simulations. This double validation procedure implies that the VSPKc model has a high reliability. The novel model highlights the importance of considering the fiber circular geometry on the estimation of elastic properties, as well as the unit cell symmetry.*

Keywords: *micromechanics of composites, effective elastic properties, analytical modeling, finite element method*

1. INTRODUCTION

Analytical models are fundamental approaches to the optimum design od composite structures due to the large amount of variables (Tsai & Melo, 2014) and multiscale characteristic (Vignoli & Savi, 2018). The present investigation is related to the microscale, where matrix and fiber properties are used to estimate the effective macromechanical response of the lamina. Considering micromechanical models, the authors have carried out an effort to compare analytical models with a set of experimental data compiled from the literature for effective elastic properties (Vignoli et al., 2019; Vignoli et al., 2021) and strengths (Vignoli et al., 2020a; Vignoli et al., 2020b).

In general, micromechanical models can be classified into three groups: models based on the Rule of Mixture (Jones, 1999); models based on the theory of elasticity (Kalamkarov, 1992); and trace-based models (Tsai et al., 2022). The ROM-based models are usually based on simple assumptions of 2D elements associated in series for the longitudinal elastic modulus, E_1, and in-plane Poisson's ratio, ν_{12}; or associated in parallel for transversal elastic modulus, E_2, and in-plane shear modulus, G_{12}. This kind of models presents good predictions for association in series, but the estimations

for associations in parallel are poor due to perturbations on the stress and strain fields related to stress concentration around the inclusions.

Other ROM-type models have been proposed to improve results for the other properties. Among these models, the most important are Halpin-Tsai (Halpin & Tsai, 1969), Chamis (Chamis et al., 2013), and the VSPK (Vignoli et al., 2019). However, these ROM modifications require calibrated parameters and do not have a solid mechanical basis. Huang et al. (2020) developed a novel model assuming square symmetry of the unit cell and octagonal geometry of fibers. The load distribution analysis considers only strength of materials hypothesis for elements associated in series or in parallel, but a considerable improvement is observed comparing with the traditional ROM using a simplified geometry.

This paper proposes a novel ROM-based model to estimate the effective elastic properties of unidirectional composites with circular cross section fibers, namely VSPKc. This model does not require calibrated parameters as the previous version of the model (VSPK) proposed by the authors. The proposed approach is the first ROM-based model able consider the real fiber cross section in a square unit cell. VSPKc predictions are compared with the classical ROM and with the model assuming fiber octagonal geometry using finite element simulations and experimental data as references. Results show good predictions using simpler equations when compared with other methods.

2. VSPKC MICROMECHANICAL MODEL

The proposed VSPKc model is a ROM-based approach to derive closed-form expressions for the effective elastic properties of unidirectional laminae. However, the main advantage of this novel model is the capability to consider a unit cell with square symmetry and the fiber circular cross section embedded in the matrix.

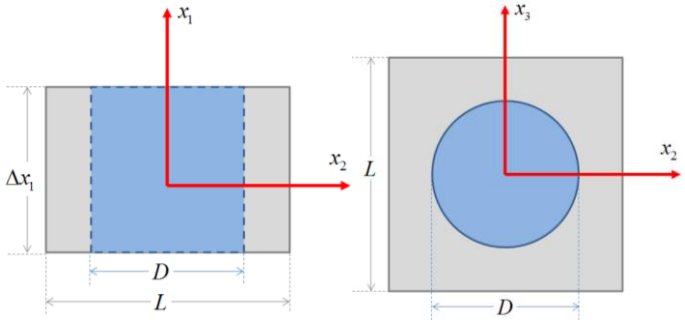

Figure 1. Unit cell with square symmetry and circular fiber.

Considering the unit cell presented in Fig. 1, the fiber's diameter is D, the unit cell length in x_2 and x_3 equal to L, the unit cell length in x_1 is equal to Δx_1. Additionally, the fiber volume fraction is $V_f = \pi D^2 / 4L^2$; consequently, $D/L = 2\sqrt{V_f/\pi}$.

Regarding the properties E_1 and ν_{12}, both fiber and matrix present the same strain. Thus, it can be assumed to be elements in parallel association that results in the classical ROM estimation can be used

$$E_1 = E_1^f V_f + E^m (1 - V_f) \tag{1}$$

$$\nu_{12} = \nu_{12}^f V_f + \nu^m (1 - V_f) \tag{2}$$

where E_1^f is the fiber longitudinal elastic modulus, ν_{12}^f is the fiber in-plane Poisson's ratio, E^m is the matrix elastic modulus, ν^m is the matrix Poisson's ratio and V_f is the fiber volume fraction.

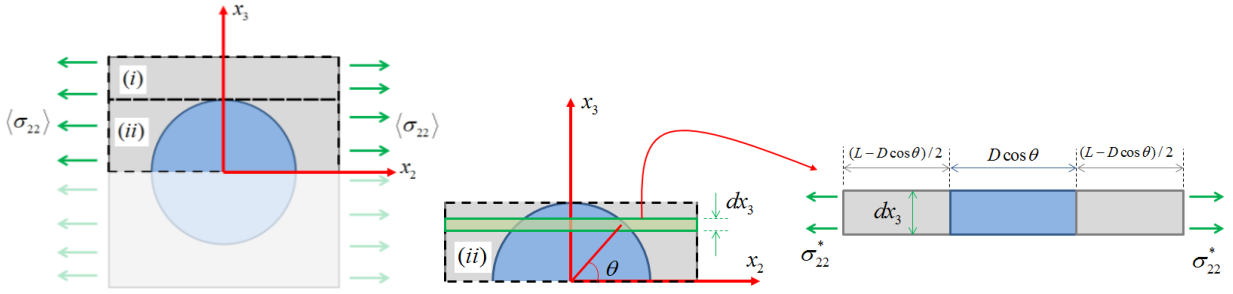

Figure 2. Transversal load applied to the unit cell.

First, a transversal load on the unit cell is considered, as shown in the Fig. 2. The unit cell is split into two regions: (i) only matrix; (ii) matrix and fiber. The proposed procedured yields a constitutive relation of the homogenized unit cell with the form $\langle\sigma_{22}\rangle = E_2\langle\varepsilon_{22}\rangle$, where $\langle\sigma_{22}\rangle$ and $\langle\varepsilon_{22}\rangle$ are the transversal stress and strain on the unit cell, respectively, and E_2 is the effective transversal elastic modulus to be obtained. Considering that regions (i) and (ii) are parallel and the unit cell is symmetric, the equilibrium requirement can be expressed by

$$\langle\sigma_{22}\rangle = \frac{2}{L}\left(\int_{D/2}^{L/2}\sigma_{22}^{(i)}dx_3 + \int_{0}^{D/2}\sigma_{22}^{(ii)}dx_3\right) \tag{3}$$

where $\sigma_{22}^{(i)}$ and $\sigma_{22}^{(ii)}$ are the stresses in regions (i) and (ii), respectively. Note that for region (i), $\sigma_{22}^{(i)}$ can be assumed independent of x_3, since there is no fiber. The matrix constitutive relation can be applied to obtain

$$\int_{D/2}^{L/2}\sigma_{22}^{(i)}dx_3 = \int_{D/2}^{L/2}E^m\varepsilon_{22}^{(i)}dx_3 = \frac{1}{2}E^m\varepsilon_{22}^{(i)}(L-D) \tag{4}$$

In region (ii), the stress $\sigma_{22}^{(ii)}$ is dependent of x_3, because there exist fiber and matrix. For the infinitesimal element shown in the Fig. 2, the stress is σ_{22}^{*}, and the strain is ε_{22}^{*}. The constitutive relation for this infinitesimal element is $\sigma_{22}^{*} = E_2^{*}\varepsilon_{22}^{*}$, where E_2^{*} is the effective elastic modulus. Realizing fiber and matrix are in series, the equilibrium requirement and geometrical compatibility are defined by:

$$\sigma_{22}^{*} = \sigma_{22}^{m} = \sigma_{22}^{f} \tag{5}$$

$$\varepsilon_{22}^{*}L = \varepsilon_{22}^{m}(L - D\cos\theta) + \varepsilon_{22}^{f}D\cos\theta \tag{6}$$

Manipulating these equations, the effective elastic modulus of this infinitesimal element can be computed by

$$E_2^{*} = E^m\left\{\frac{1}{1+2[(E^m/E_2^f)-1]\sqrt{V_f/\pi}\cos\theta}\right\} \tag{7}$$

Once E_2^{*} is obtained, the stress integral of region (ii) can be expressed by

$$\int_{0}^{D/2}\sigma_{22}^{(ii)}dx_3 = \int_{0}^{D/2}E^{*}\varepsilon_{22}^{(ii)}dx_3 = E^m\varepsilon_{22}^{(ii)}\int_{0}^{D/2}\left\{\frac{1}{1+2[(E^m/E_2^f)-1]\sqrt{V_f/\pi}\cos\theta}\right\}dx_3 \tag{8}$$

The integral presented in Eq. (8) is calculated by using MATLAB and the following expression is derived:

$$\int_{0}^{D/2}\sigma_{22}^{(ii)}dx_3 = E^m\varepsilon_{22}^{(ii)}\frac{D}{2}\left[\frac{\pi}{2a_{22}} - \frac{\ln\left(a_{22}+\sqrt{a_{22}^{\,2}-1}\right)}{a_{22}\sqrt{a_{22}^{\,2}-1}}\right] \tag{9}$$

where $a_{22} = 2[(E^m/E_2^f)-1]\sqrt{V_f/\pi}$.

Using Eqs.(4) and (9) into Eq. (3) and assuming that $\langle\varepsilon_{22}\rangle = \varepsilon_{22}^{(i)} = \varepsilon_{22}^{(ii)}$ by geometrical compatibility, the effective transversal modulus is:

$$E_2 = E^m\left\{1+2\sqrt{\frac{V_f}{\pi}}\left[\frac{\pi}{2a_{22}}-\frac{\ln\left(a_{22}+\sqrt{{a_{22}}^2-1}\right)}{a_{22}\sqrt{{a_{22}}^2-1}}-1\right]\right\} \tag{10}$$

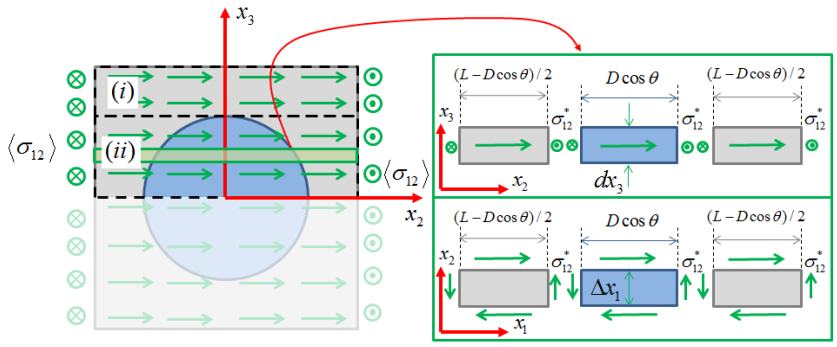

Figure 3. In-plane shear load applied to the unit cell.

The estimation of the in-plane shear modulus is based on unit cell presented in Fig. 3 and the goal is to stablish the constitutive relation for in-plane shear load: $\langle\sigma_{12}\rangle = 2G_{12}\langle\varepsilon_{12}\rangle$. The equilibrium requirement is defined by

$$\langle\sigma_{12}\rangle = \frac{2}{L}\left(\int_{D/2}^{L/2}\sigma_{12}^{(i)}dx_3 + \int_{0}^{D/2}\sigma_{12}^{(ii)}dx_3\right) \tag{11}$$

The integral of shear stress in region (i), where there is only matrix, is

$$\int_{D/2}^{L/2}\sigma_{12}^{(i)}dx_3 = \int_{D/2}^{L/2}2G^m\varepsilon_{12}^{(i)}dx_3 = G^m\varepsilon_{12}^{(i)}(L-D) \tag{12}$$

The following expression is obtained from the procedure similar to the one used for the effective transversal elastic modulus for the infinitesimal region shown in Fig. 3:

$$G_{12}^* = G^m\left\{\frac{1}{1+2[(G^m/G_{12}^f)-1]\sqrt{V_f/\pi}\cos\theta}\right\} \tag{13}$$

Hence, the integral of region (ii) in Eq. (11) is

$$\int_{0}^{D/2}\sigma_{12}^{(ii)}dx_3 = \int_{0}^{D/2}2G_{12}^*\varepsilon_{12}^{(ii)}dx_3 = G^m\varepsilon_{12}^{(ii)}D\int_{0}^{D/2}\left\{\frac{1}{1+a_{12}\cos\theta}\right\}dx_3 \tag{14}$$

where $a_{12} = 2[(G^m/G_{12}^f)-1]\sqrt{V_f/\pi}$. Note that this integral is similar to the one discussed in Eq. (8). Using the same symbolic solution, Eq. (14) can be rewritten as:

$$\int_{0}^{D/2}\sigma_{12}^{(ii)}dx_3 = G^m\varepsilon_{12}^{(ii)}D\left[\frac{\pi}{2a_{12}}-\frac{\ln\left(a_{12}+\sqrt{{a_{12}}^2-1}\right)}{a_{12}\sqrt{{a_{12}}^2-1}}\right] \tag{15}$$

Considering that regions (i) and (ii) are parallel, $\langle\varepsilon_{12}\rangle = \varepsilon_{12}^{(i)} = \varepsilon_{12}^{(ii)}$. Using this compatibility condition and applying Eqs. (12) and (15) into the Eq. (11), the effective in-plane shear modulus is:

$$G_{12} = G^m \left\{ 1 + 2\sqrt{\frac{V_f}{\pi}} \left[\frac{\pi}{2a_{12}} - \frac{\ln\left(a_{12} + \sqrt{{a_{12}}^2 - 1} \right)}{a_{12}\sqrt{{a_{12}}^2 - 1}} - 1 \right] \right\}, \tag{16}$$

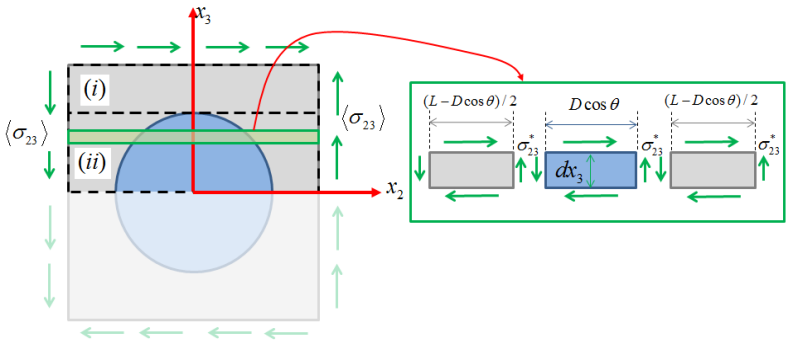

Figure 4. Out-of-plane shear load applied to the unit cell.

Out-of-plane shear modulus G_{23} is now in focus considering an out-of-plane load to obtain the constitutive model $\langle\sigma_{23}\rangle = 2G_{23}\langle\varepsilon_{23}\rangle$. Comparing both shear loads presented in Figs. 3 and 4, it can be realized that they are similar. The main difference is the plane where the elements are assumed in parallel. The equilibrium requirement for out-of-plane shear load is defined by:

$$\langle\sigma_{23}\rangle = \frac{2}{L}\left(\int_{D/2}^{L/2} \sigma_{23}^{(i)} dx_3 + \int_{0}^{D/2} \sigma_{23}^{(ii)} dx_3 \right) \tag{17}$$

Integrating the out-of-plane of shear stress in regions (i) and (ii), the following expression are obtained:

$$\int_{D/2}^{L/2} \sigma_{23}^{(i)} dx_3 = \int_{D/2}^{L/2} 2G^m \varepsilon_{23}^{(i)} dx_3 = G^m \varepsilon_{23}^{(i)} (L - D) \tag{18}$$

$$\int_{0}^{D/2} \sigma_{23}^{(ii)} dx_3 = \int_{0}^{D/2} 2G_{23}^{*} \varepsilon_{23}^{(ii)} dx_3 = G^m \varepsilon_{23}^{(ii)} D \int_{0}^{D/2} \left\{ \frac{1}{1 + a_{23}\cos\theta} \right\} dx_3 = G^m \varepsilon_{23}^{(ii)} D \left[\frac{\pi}{2a_{23}} - \frac{\ln\left(a_{23} + \sqrt{{a_{23}}^2 - 1} \right)}{a_{23}\sqrt{{a_{23}}^2 - 1}} \right] \tag{19}$$

where $a_{23} = 2[(G^m / G_{23}^f) - 1]\sqrt{V_f / \pi}$.

Considering $\langle\varepsilon_{23}\rangle = \varepsilon_{23}^{(i)} = \varepsilon_{23}^{(ii)}$ since regions (i) and (ii) are parallel, the formula for the effective out-of-plane shear modulus is:

$$G_{23} = G^m \left\{ 1 + 2\sqrt{\frac{V_f}{\pi}} \left[\frac{\pi}{2a_{23}} - \frac{\ln\left(a_{23} + \sqrt{{a_{23}}^2 - 1} \right)}{a_{23}\sqrt{{a_{23}}^2 - 1}} - 1 \right] \right\} \tag{20}$$

3. FINITE ELEMENT METHOD

The finite element method (FEM) model is built by considering the same essential hypothesis of the analytical model: composite behavior is based on the unit cell. Therefore, FEM model considers unit cells based on the fiber volume fraction. Ansys software is employed considering a quadratic and three-dimensional element: SOLID186. The unit cell is built considering the same fiber diameter and hence, different fiber volume fraction is represented by different unit cell size. Fiber and matrix are assumed to be perfectly bonded and the multi-point constraint formulation is applied. Seven

situations are analyzed, being represented by different fiber volume fractions V_f : 0.1, 0.2, 0.3, 0.4, 0.5, 0.6, 0.7. Fiber diameter D and cell size Δx_1 are kept constants, $L = \sqrt{\pi D^2 / 4V_f}$, as illustrated in Fig. 5 that also shows the mesh details obtained after a convergence analysis. Table 1 presents details about the meshes.

Periodic boundary conditions are imposed, being mathematically expressed by

$$U_i^{(J+)} - U_i^{(J-)} = \lambda_j^{(J)} \tag{21}$$

where $\lambda_i^{(J)}$ is a constant parameter that represents the difference between displacements of faces $J+$ and $J-$ in i direction, $U_i^{(J+)}$ and $U_i^{(J-)}$, respectively.

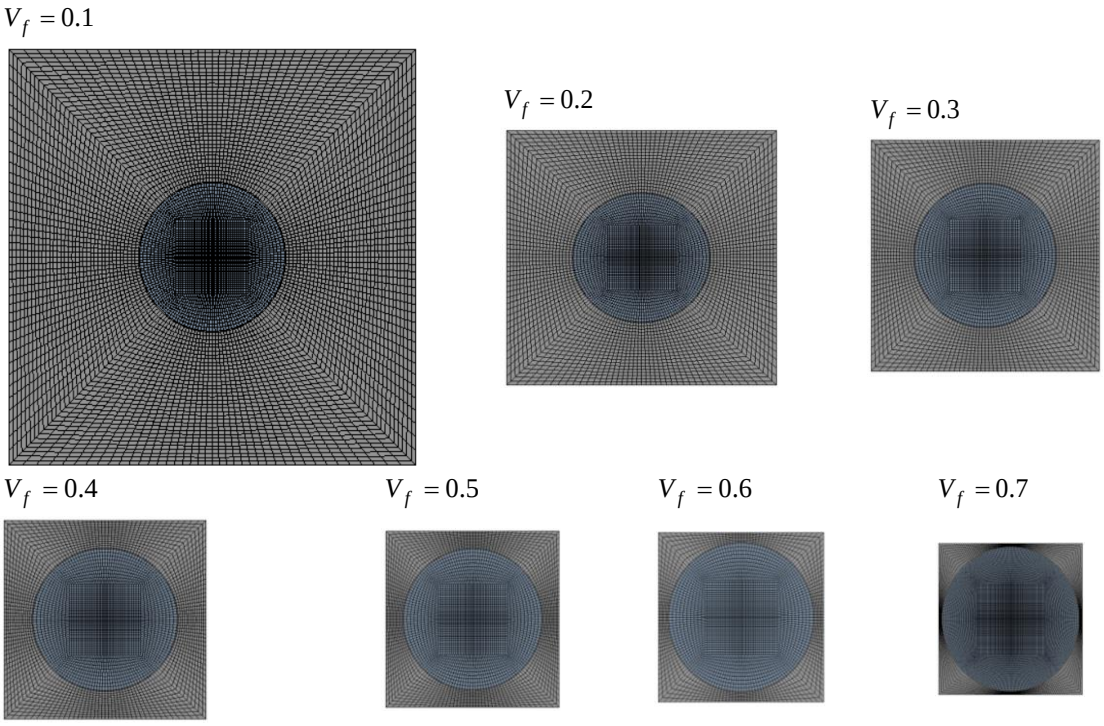

Figure 5. FEM meshs for $0.1 \le V_f \le 0.7$

Table 1. Number of elements and nodes for FEM simulations.

V_f	0.1	0.2	0.3	0.4	0.5	0.6	0.7
Elements	8960	6560	5760	5440	5280	4480	14925
Nodes	63923	47123	41523	39283	38163	32563	106728

4. RESULTS AND DISCUSSION

Results of the proposed VSPKc model are discussed in this Section in two different ways comparing VSPKc predictions with two other models available in the literature: ROM (Jones, 1999) and octagonal fibers model (Oct) (Huang et al., 2020). Equations of these models are omitted, but they can be obtained on the quoted references. Finite element method (FEM) is employed for model verification. Additionally, a set of 126 compiled experimental data for carbon and glass fibers and epoxy matrices (Vignoli et al. 2022).

For the FEM, a composite made by an epoxy matrix with $E^m = 3.2\text{GPa}$, $\nu^m = 0.35$ and carbon fibers with $E_1^f = 231\text{GPa}$, $E_2^f = 15\text{GPa}$, $G_{12}^f = 15\text{GPa}$, $G_{23}^f = 7\text{GPa}$, and $\nu_{12}^f = 0.2$ is considered. Figure 6 shows the comparison between the analytical models and the FEM results for E_1 . The three analytical models use the same equation for E_1 , Eq.(1). Results indicate that the error tends to zero and a simple equation is accurate to estimate this property. Results for ν_{12} are presented in Fig. 7 and no considerable difference is achieved, despite Oct model uses an equation slightly different than Eq.(2).

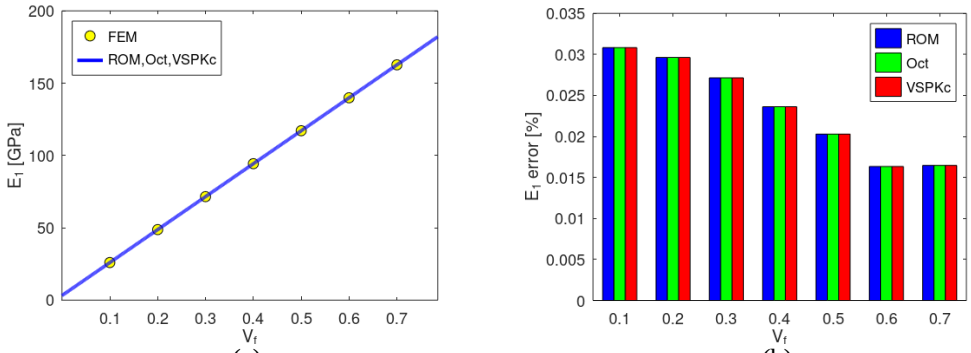

(a) (b)

Figure 6. Comparison between analytical estimations and FEM results for E_1: a) influence of V_f; b) absolute error.

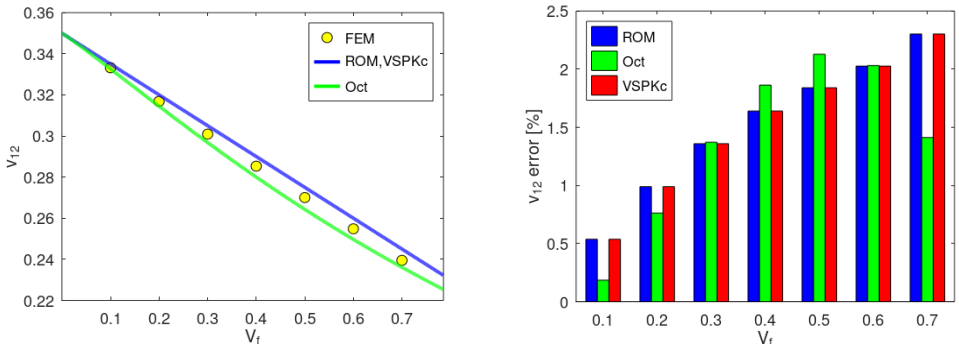

(a) (b)

Figure 7. Comparison between analytical estimations and FEM results for ν_{12}: a) influence of V_f; b) absolute error.

The results for E_2 are presented in Fig. 8, indicating that VSPKc has the best prediction compared with FEM. Results of the classical ROM presents error ranges between 13.6% and 28.2%; Oct model presents error ranges between 12.7% and 22%; VSPKc error ranges are between 12.2% and 17.1%. Additionally, the error tends to increase when V_f for ROM, while there is a small variation for the VSPKc model.

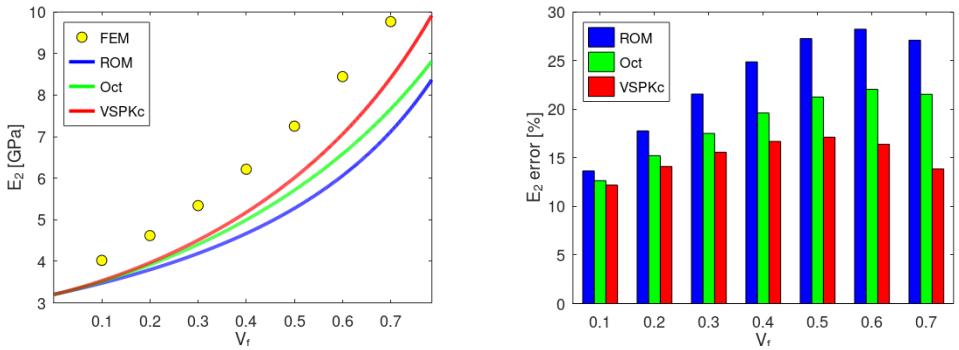

(a) (b)

Figure 8. Comparison between analytical estimations and FEM results for E_2: a) influence of V_f; b) absolute error.

Figure 9 shows the results for G_{12}. The ROM has error ranges between 7.2% and 37.1%; Oct has error ranges between 5% and 12.7%; VSPKc presents error ranges between 4.9% and 8.3%. Once again, VSPKc model has the best estimation for any V_f.

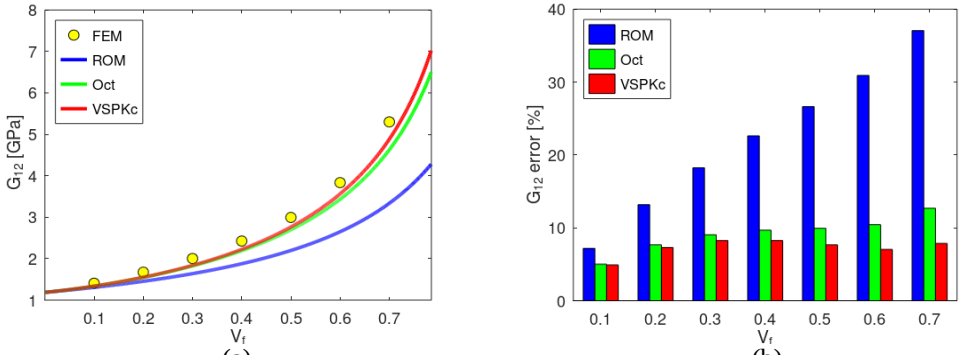

Figure 9. Comparison between analytical estimations and FEM results for G_{12}: a) influence of V_f; b) absolute error.

The results for G_{23} are presented in Fig. 10, showing that: ROM estimations has error ranges between 17.4% and 37.6%; Oct presents error ranges between 2.8% and 16.2%; on the other hand, VSPKc has error ranges between 2.7% and 14%. VSPKc model has the best estimation for any V_f again and these results indicate a considerable improvement due to the capability to model the actual fiber circular cross section.

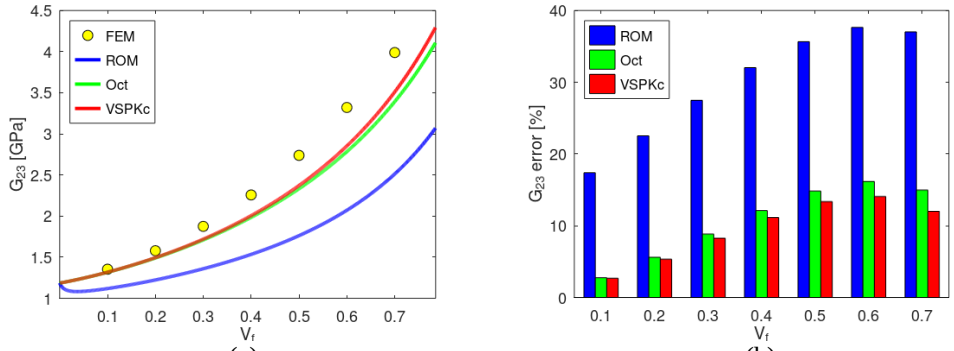

Figure 10. Comparison between analytical estimations and FEM results for G_{23}: a) influence of V_f; b) absolute error.

A set of 126 compiled experimental results are now evaluated to verify the different models. This set has: 54 data for E_2, 46 data for G_{12} and 26 data for G_{23}. Just the estimations of E_2, G_{12} and G_{23} are compared because the estimations of E_1 and ν_{12} are very similar. Figure 11 shows the comparison of ROM, Oct, and VSPKc predictions. The modeling improvement to consider the fiber cross section influence has a considerable influence on the results. Once again, VSPKc obtained the closest prediction, followed by Oct, and the worst predictions are by ROM. The novel VSPKc model presents the following average errors: 12.9% for G_{23}, 16.4% for G_{12} and 17.1% for E_2. These results indicate that the VSPKc has reliable estimations with a simple set of equations without any calibration parameter.

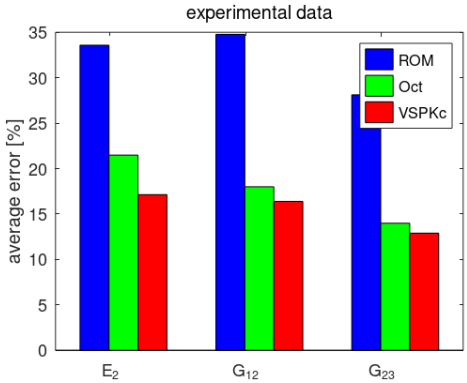

Figure 11. Average errors for the effective properties E_2, G_{12}, and G_{23} of the analytical models compared with the experimental data.

5. CONCLUSIONS

This paper presents the derivation of a novel ROM-based micromechanical model considering the elastic unidirectional composites with circular cross section fibers. The main advantage of the VSPKc model is that it requires only 8 explicit analytical formulas and does not require any experimentally calibrate parameters. Results show the importance of accounting the fiber geometry in order to improve the accuracy of the effective properties, which is carried out assuming a square unit cell. This conclusion is confirmed by comparisons with other analytical models, ROM and Oct, with FEM results and with a large number of experimental data.

6. ACKNOWLEDGEMENTS

The authors would like to acknowledge the support of the Brazilian Research Agencies CNPq, CAPES, FAPERJ and the Natural Sciences and Engineering Research Council of Canada (NSERC).

7. REFERENCES

Chamis, C.C., Abdi, F., Garg, M., Minnetyan, L., Baid, H., Huang, D., Housner, J., Talagani, F., 2013, Micromechanics-based progressive failure analysis prediction for WWFE-III composite coupon test cases, J Compos Mater, 47, 2695–2712.

Halpin, J.C., Tsai, S.W, 1969, Effects of environmental factors on composite materials, AFML-TR, 67,423.

Huang, Y., Cimini Jr, C.A., Ha, S.K., 2020, A micromechanical unit cell model with an octagonal fiber for continuous fiber reinforced composites, Journal of Composite Materials, 54, 4495–4513.

Jones, R.M., 1999, Mechanics of composite materials, 2 ed., Taylor & Francis.

Kalamkarov, A.L., 1992, Composite and reinforced elements of construction, Wiley.

Tsai, S.W., Melo, J.D.D., An invariant-based theory of composites, Compos Sci Technol, 100, 237–243.

Tsai, S.W., et al., 2022, DOUBLE–DOUBLE A New Perspective in The Manufacture and Design of Composites, Composite Design Group, Stanford.

Vignoli, L.L., Savi, M.A., 2018, Multiscale Failure Analysis of Cylindrical Composite Pressure Vessel: A Parametric Study, Latin American Journal of Solids and Structures, 15, 1-20.

Vignoli, L.L., Savi, M.A., Pacheco, P.M.C.L., Kalamkarov, A.L., 2019, Comparative analysis of micromechanical models for the elastic composite laminae, Composites Part B, 174, 106961.

Vignoli, L.L., Savi, M.A., Pacheco, P.M.C.L., Kalamkarov, A.L., 2020a, Micromechanical analysis of transversal strength of composite laminae, Composite Structures, 250, 112546.

Vignoli, L.L., Savi, M.A., Pacheco, P.M.C.L., Kalamkarov, A.L., 2020b, Micromechanical analysis of longitudinal and shear strength of composite laminae, Journal of Composite Materials, 54, 4853-4873.

Vignoli, L.L., Neto, R.M.C., Savi, M.A., Pacheco, P.M.C.L., Kalamkarov, A.L., 2021, Trace Theory Applied to Composite Analysis: A Comparison with Micromechanical Models, Composites Communications, 25, 100715.

Vignoli, L.L., Savi, M.A., Pacheco, P.M.C.L., Kalamkarov, A.L., 2022, A Novel Micromechanical Model Based on the Rule of Mixtures to Estimate Effective Elastic Properties of Circular Fiber Composites, Applied Composite Materials, 29, 1715–1731.

8. RESPONSIBILITY NOTICE

The authors are the only responsible for the printed material included in this paper.